Proceedings of Ninth World Conference on Earthquake Engineering
August 2-9, 1988, Tokyo-Kyoto, JAPAN (Vol.III)

5-2-11

NONLINEAR VIBRATION ANALYSIS OF UPLIFTING RIGID BODIES ON AN ELASTIC HALFSPACE

Yukio SHIMOMURA[1] and Hiroshi TAJIMI[2]

[1]Department of Architecture, Nihon University, Chiyoda-ku, Tokyo, Japan

[2]Emeritus Professor, Nihon University, Chiyoda-ku, Tokyo, Japan

SUMMARY

A numerical method for obtaining uplifting foundation response due to earthquake inputs is presented. The method assumes that the foundation rests on an elastic halfspace and is based on the time dependent Green's function. The dynamic subgrade stiffness for an uplifting massless rigid foundation subjected to sinusoidal excitation is linearly approximated as the equivalent complex stiffness(ECS). Applying the ECS to a lumped parameter model, a practical calculation procedure to determine the frequency transfer function for uplifting rigid bodies is proposed.

INTRODUCTION

Recently, many studies have been carried out on the nonlinear vibration of structures induced by uplifting. The majority of these analyses are based on lumped parameter models. When estimating model constants, it is advisable to calculate the dynamic subgrade stiffness(DSS) for an uplifting foundation in order to respect the semi-infinite nature of the supporting soil. However, due primarily to the difficulty of calculation, the DSS is often not determined. Wolf et. al.(Ref.1) proposed a nonlinear soil-structure interaction analysis procedure, which is based on the boundary element method with the impulsive Green's function. The function is first calculated in the frequency domain and then approximately transformed into the time domain by the FFT method. However, their procedure required a large computational effort and there was no specific mention of DSS. Kawakami et. al.(Ref.2) calculated the DSS by a hybrid frequency-time domain procedure. Unfortunately, the solutions are often non convergent.

We propose a simplified numerical procedure based on the impulsive Green's function for an elastic halfspace, which is directly calculated in the time domain but not as in Ref.1. By analyzing an uplifting massless rigid foundation subjected to sinusoidal excitation, the DSS is determined using the equivalent linearization method and is defined as the equivalent complex stiffness(ECS). Using the above ECS, a practical calculation for the frequency transfer function of a rigid body subjected to sinusoidal earthquake-like inputs is demonstrated.

TIME DEPENDENT DISPLACEMENT FUNCTIONS FOR A CONCENTRATED UNIT-STEP LOAD

It is assumed that the supporting soil is a homogeneous elastic halfspace which can be described by a cylindical coordinate system (r,θ,z) as shown in

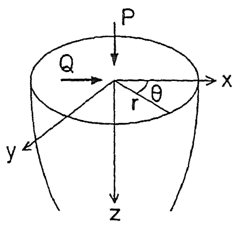

Fig.1 Coordinate system

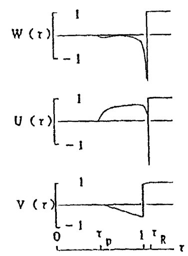

Fig.2 $W(\tau)$, $U(\tau)$ and $V(\tau)$ where $\nu = 0.45$

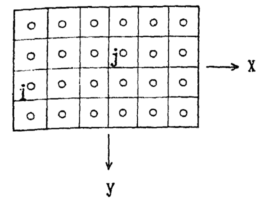

Fig.3 Discrete model of foundation area

Fig.1. Whwn a vertical point load, $PH(t)$, is applied at the origin, the vertical displacement of an arbitrary point on the soil surface is written as follows, where $H(t)$ is a unit step function(Refs.3 and 5).

$$w(r,t) = \frac{1-\nu}{2\pi G}\frac{P}{r}W(\tau) \tag{1}$$

The horizontal displacement in the x-direction at a given point (r,θ,z) caused by a point load, $QH(t)$, in the x-direction at the origin is also written

$$u(r,\theta,t) = \frac{1}{2\pi G}\frac{Q}{r}[U(\tau)\cos^2\theta + (1-\nu)V(\tau)\sin^2\theta] \tag{2}$$

where ν=the Poisson's ratio and G=the shear modulus(Refs.4 and 5). τ is the dimensionless time $V_s t/r$, where V_s is the shear wave velocity of the medium.

$W(\tau)$, $U(\tau)$ and $V(\tau)$ denote the time dependent terms of the displacement functions as shown in Fig.2, where $\nu=0.45$. These are equal to 1 for $\tau \geq \tau_R = V_s/V_R$, where V_R is the Rayleigh wave velocity of the medium.

NODAL DISPLACEMENT OF SOIL SURFACE

The soil surface displacement for vertical point loading P(t) applied at the origin is obtained using the temporal Duhamel's integration as follows.

$$w(r,t) = \frac{1-\nu}{2\pi Gr}\{P(t)W(0) + \int_0^t P(t-t')\frac{dW}{dt'}dt'\} = \frac{1-\nu}{2\pi Gr}\{P(t)W(0) + \int_0^t P(t-t')\Delta W(\frac{V_s t'}{r})\} \tag{3}$$

The foundation area, the soil surface below the foundation, is discretized by numerous mesh elements, and a node is located at the center of each element. It is assumed that the surface traction within an element is uniformly distributed and is constant over a short time interval, Δt. The nodal force is defined by the resultant surface traction within the corresponding element. On the n-th time step$(n\Delta t<t\leq(n+1)\Delta t)$, the increment of the vertical displacement of the i-th node, Δw^s_{in} can be represented to incorporate all nodal forces acting on the foundation area.

$$\Delta w^s_{in} = w_{sii}\Delta p_{in} + \sum_{j=1}^{N}(1-\delta_{ij})w_{sij}\sum_{m=0}^{m'}\Delta p_{j(n-m)}H^W_{ijm} \tag{4}$$

Where N=the total number of nodes, p_{jn}=the vertical component of the j-th nodal force at the n-th step, Δp_{jn}=the increment of p_{jn}, m'= the minimum integer satisfying $H^W_{ijm}=0$, δ_{ij}=Kronecker's delta symbol, and H^W_{ijm} is defined below

$$H^W_{ijn} = W_{ijn} - W_{ij(n-1)} \tag{5}$$

where,

$$W_{ijn} = \frac{1-\nu}{2\pi G}\frac{1}{\Delta t(\Delta L)^2}\int_{n\Delta t}^{(n+1)\Delta t}\int_{-\frac{\Delta L}{2}}^{\frac{\Delta L}{2}}\int_{-\frac{\Delta L}{2}}^{\frac{\Delta L}{2}}\frac{1}{r}W(\frac{V_s t}{r})dx'_j dy'_j dt\,\frac{1}{w_{sij}} \tag{6}$$

where r=the distance between the i-th and j-th nodes, and w_{sij} is the i-th nodal displacement for a unit static load within the j-th element and is a given.

$$w_{sij} = \frac{1-\nu}{2\pi G}\frac{1}{(\Delta L)^2}\int_{-\frac{\Delta L}{2}}^{\frac{\Delta L}{2}}\int_{-\frac{\Delta L}{2}}^{\frac{\Delta L}{2}}\frac{1}{r}dx'_j dy'_j \tag{7}$$

Eq.(4) can be rewritten in matrix form as follows

$$\{\Delta w^s\}_n=[\alpha_v]_o\{\Delta p\}_n+\sum_{m=1}^{m}[\alpha_v]_m\{\Delta p\}_{n-m}=[\alpha_v]_o\{\Delta p\}_n+\{\Delta w^p\}_n \tag{8}$$

where elements of $[\alpha_v]_m$ are provided by Eqs.(5)-(7). $\{\Delta w^p\}_n$ is the increment of the nodal displacement vector produced by wave propagation due to the past loading in the foundation area and is a known value.

In the case of horizontal loading, the n-th step increment of the nodal displacement vector $\{\Delta u^s\}_n$ in the y-direction is also derived as below,

$$\{\Delta u^s\}_n=[\alpha_H]_o\{\Delta q\}_n+\sum_{m=1}^{m'}[\alpha_H]_m\{\Delta q\}_{n-m}=[\alpha_H]_o\{\Delta q\}_n+\{\Delta u^p\}_n \tag{9}$$

where $\{\Delta q\}_n$=the increment of the nodal force vector in the y-direction.

RELATIONSHIP BETWEEN REACTIVE FORCE AND FOUNDATION DISPLACEMENT

The bottom surface of the foundation is discretized by mesh elements in the same manner as with the soil surface below the foundation. When a vertical static load P and an exciting moment M(t) about the x-axis are applied at the center of a massless rigid foundation, the independent kinematic quantities of the foundation are expressed by the vertical displacement and the angular rotation about the x-axis at the center. Here, these quantities are defined by w_n^f and θ_n^f respectively for the n-th time step. The displacement of an arbitrary point of the foundation can be given as a function of these independent quantities.

Since there is no tension between the foundation and the soil surface, partial uplift can occur. The foundation area is devided into a contact-region and an uplift-region, when the foundation is uplifting. The nodal displacement of the soil surface within the contact-region is equal to that of the foundation. While in the uplift-region, they are not equal and no surface traction occurs. Therefore, the resultant reactive forces for the foundation are expressed by the nodal force vector.

$$P_n=\{1\}^T\{p\}=\{\hat{1}\}^T\{\hat{p}\} \quad , \quad M_n=\{y\}^T\{p\}=\{\hat{y}\}^T\{\hat{p}\} \tag{10}$$

Where the notation ˆ indicates matrices and vectors for contact nodes, and vector {y} consists of the nodal coordinate values in the y-direction.

The nodal displacement vector of the soil surface is derived from Eq.(8) and is written as follows.

$$\{w^s\}_n=[\alpha_v]_o\{p\}_n+\{w^p\}_n \tag{11}$$

The above equation is represented in consideration of the boundary conditions as below.

$$\{\hat{w}^s\}_n=\{\hat{w}^f\}_n=w_n^f\{\hat{1}\}+\theta_n^f\{\hat{y}\}=[\hat{\alpha}_v]_o\{\hat{P}\}_n+\{\hat{W}^p\}_n \tag{12}$$

Conversely, the nodal force vector is written as follows.

$$\{\hat{p}\}_n=[\hat{\alpha}_v]_o^{-1}(\{\hat{w}^s\}_n-\{\hat{w}^p\}_n) \tag{13}$$

Substituting Eqs.(12) and (13) into Eq.(10) leads to

$$\begin{bmatrix} P_n \\ M_n \end{bmatrix}=\begin{bmatrix} \hat{K}_{vv} & \hat{K}_{v\theta} \\ \hat{K}_{\theta v} & \hat{K}_{\theta\theta} \end{bmatrix}\begin{bmatrix} w_n^f \\ \theta_n^f \end{bmatrix}-\begin{bmatrix} P_n^p \\ M_n^p \end{bmatrix} \tag{14}$$

where

$$\hat{K}_{vv}=\{\hat{1}\}^T[\hat{k}_v]_o\{\hat{1}\} \;, \quad \hat{K}_{v\theta}=\hat{K}_{\theta v}=\{\hat{1}\}^T[\hat{k}_v]_o\{\hat{y}\} \;, \quad \hat{K}_{\theta\theta}=\{\hat{y}\}^T[\hat{k}_v]_o\{\hat{y}\}$$

$$P_n^p=\{\hat{1}\}^T[\hat{k}_v]_o\{\hat{w}^p\}_n, \quad M_n^p=\{\hat{y}\}^T[\hat{k}_v]_o\{\hat{w}^p\}_n \;, \quad [\hat{k}_v]_o=[\hat{\alpha}_v]_o^{-1} \tag{15}$$

The unknowns, w_n^f, θ_n^f and $\{w^s\}_n$ can be obtained from Eqs.(14), (12) and (11) by the iterative calculation for these terms.

Corresponding nodes for the foundation and soil have the same motion providing that they have not been separated due to uplifting. But, each has a different motion during separation, and the horizontal dislocation between the two nodes generally remains after uplifting. Therefore, the horizontal displacement of the foundation for a horizontal excitation must be calculated in consideration of this dislocation.

EQUIVALENT COMPLEX STIFFNESS

When a massless rigid foundation is subjected to a vertical static load P, an exciting moment, $M\sin\omega t$, about the x-axis and an exciting force, $Q\sin\omega t$, in the y-direction, the foundation displacement can be computed by the procedure mentioned in the former section. The time histories of the angular rotation about the x-axis and the displacement in the y-direction of the foundation become a steady state shortly after the initial excitation. Considering one cycle of this steady state, each of these time histories is expanded to a Fourier series. The series has higher-order frequency components which are odd numbered harmonics of the excitation frequency. The angular rotation, $\theta^f(t)$, can be expressed in complex form, as below.

$$\theta^f = \Theta_1 e^{i(\omega t-\phi_1)} + \Theta_3 e^{i(3\omega t-\phi_3)} + \Theta_5 e^{i(5\omega t-\phi_5)} + \cdots \tag{16}$$

As $\Theta_1 >> \Theta_3 > \Theta_5 >$, the angular rotation can be approximated by the term Θ_1. Using the same complex expression for the exciting moment, the DSS associated with the rocking mode can be approximated as the ECS, which is represented by the ratio of the exciting moment to the approximate angular rotation, as follows.

$$K_\theta + iK'_\theta = \frac{M}{\Theta_1} e^{i\phi_1} \tag{17}$$

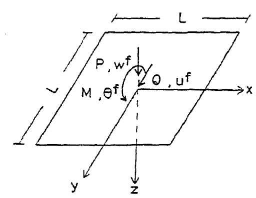

Fig.4 Massless rigid foundation

The equation for the ECS associated with the swaying mode is similar to that shown in Eq.(17).

Numerical Model Soil: V_s=100m/sec. G=1500tf/m^2, ν=0.45, mass density; ρ_s=0.15 tfs^2/m^4. Massless Rigid Foundation: LxL=10mx10m square and the area is discretized by 10x10 mesh elements. Further, the time interval Δt=1/100sec and the vertical static load P=1000tf.

Results and Discussion From the preliminary calculation of uplifting foundation response due to the static moment about the x-axis, it was found that the critical moment M_c can be approximated by PL/5. Further, it was found that the reduction in the secant modulus of the static subgrade stiffness associated with the rocking mode which accompanies uplift can be approximated by the equation

$$f(\eta) = \eta^{\frac{5}{4}}\left(\frac{9}{4} - \frac{5}{4}\eta\right) \tag{18}$$

where η=the contact ratio. Fig.5 shows the relationship between the excitation frequency ω and the contact ratio η, when the range for M/M_c is 1-2. From this figure, it is evident that the influence of ω on η can be omitted. Figs.6 and 7 show the ECS. From these figures, the following conclusions can be drawn when the uplifted area is relatively small(contact ratio η>0.5).

(1)The ECS associated with the rocking mode, $K_\theta(\omega,\eta)$, can be expressed by separating the variables ω and η.

$$K_\theta(\omega,\eta) = f(\eta)[K_{\theta e}(\omega) + iK'_{\theta e}(\omega)] \tag{19}$$

where $K_{\theta e}(\omega)$ and $K'_{\theta e}(\omega)$ respectively indicate the real and imaginary parts of the complex stiffness for the linear case, i.e. no uplift.
Consequently, the effect of η on the equivalent damping ratio associated with the rocking mode is extremely small.

(2)Neither the real nor imaginary part of the ECS associated with the swaying mode is significantly influenced by η; that is

$$K_H(\omega,\eta) = K_{He}(\omega) + iK'_{He}(\omega) \tag{20}$$

where $K_{He}(\omega)$ and $K'_{He}(\omega)$ respectively indicate the real and imaginary parts of the complex stiffness for the linear case.

The equation of motion of a rigid body subjected to the y-directional horizontal earthquake inputs, shown in Fig.8, is written as follows;

$$[m]\{\ddot{u}\}+\{R\}=\{f\} \qquad (21)$$

where

$$[m]=\left[\begin{array}{cc:c} m & m\frac{H}{2} & \\ m\frac{H}{2} & J_o+m(\frac{H}{2})^2 & \\ \hdashline & & m \end{array}\right], \quad \{u\}=(u^f,\theta^f,w^f)^T, \quad \{R\}=(R_H,R_\theta,R_V)^T, \quad \{f\}=m(-\ddot{u}_g,-\frac{H}{2}\ddot{u}_g,g)^T$$

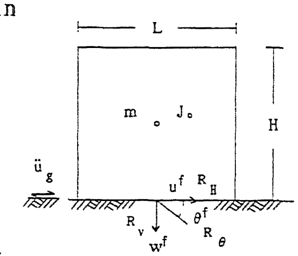

Fig.8 Rigid body

and where g=the acceleration of gravity.

It is assumed that $u_g=U_g e^{i\omega t}$ and the vertical acceleration, $\ddot{w}^f$, induced by uplifting can be omitted. Taking account of the steady state response, it is also assumed that $u^f=U^f e^{i\omega t}$ and $\theta^f=\Theta^f e^{i\omega t}$. Further, using the approximations shown in Eqs. (19) and (20) for the ECS, Eq.(21) is represented as below

$$(-\omega^2[M]+[K])\{U\}e^{i\omega t}=\omega^2 U_g\{F\}e^{i\omega t} \qquad (22)$$

where [M]=the sub-matrix of [m] denoted by the dotted line, $\{U\}=(U^f,\Theta^f)^T$ and $\{F\}=(m, m/H)^T$.

Furthermore, considering the resonance frequency of the system, ω_r, in the linear case, the complex stiffness is represented by a simple device consisting of a static spring with added mass and dashpot; but the added mass in the swaying mode can be omitted. Then, [K] is expressed as follows.

$$[K]=\mathrm{diag.}\,(K_{He}(0)+iK'_{He}(\omega_r),\ f(\eta)(K_{\theta e}(0)-\omega^2 J_a+iK'_{\theta e}(\omega_r))) \qquad (23)$$

Fixing the values of ω and η, U_g and U^f can be calculated by Eq.(22), and Θ^f is *calculated from* η *as below,*

$$\eta=[\theta_c/\Theta]^{\frac{4}{5}}\ (\text{when }\Theta>\theta_c),\qquad \eta=1\ (\text{when }\Theta\leqq\theta_c) \qquad (24)$$

where θ_c is the critical rocking angle for the static load $mgL/5K_{\theta e}(0)$.

Generally, η is calculated from $|\ddot{u}_g|$ when ω is fixed, but is difficult to obtain directly because η is a multiple-valued function of $|\ddot{u}_g|$. While, $|\ddot{u}_g|$ is a single-valued function of η and can be easily calculated. Therefore, in this study, the relationship of η vs. $|\ddot{u}_g|$ is determined for some specific values of η, as shown in Fig.9. In the uni-valued portion of the graph(i.e.), the relationship is the same regardless whether the excitation frequency increases, decreases or is step sinusoidal. For the multi-valued section of the graph, the solid line represents the increasing frequency and step sinusoidal case, the dot-dash line the instability zone and the broken line the case for decreasing frequency. By using the soild line portion of the relationship η vs. $|\ddot{u}_g|$, a value of η can be obtained from a given value of $|\ddot{u}_g|$ by the bi-section method, since the input motion is considered here to be step sinusoidal.

<u>Results</u> <u>and</u> <u>Discussion</u> The numerical example is the same as one in the former section. Further, the rigid body is a solid, where the mass density, $\rho_b=\rho_s/4$ and the height, H=1.5L.

The magnification factor of the horizontal acceleration at the top of the rigid body $|\ddot{u}_T/\ddot{u}_g|$ is shown in Fig.10, and the corresponding contact ratio is shown in Fig.11. In these figures, the solid lines show the approximate results and the symbols show the detailed results from Eq.(21). These are in good agreement with each other within the uplifting range of $\eta>0.5$.

CONCLUSION

The equivalent radiation damping ratios associated with both rocking and swaying modes do not significantly change even if the uplift area is nearly equal to the contact area. Further, the lumped parameter model based on the ECS is effective for the practical calculation of the frequency transfer function, and we feel the detailed method presented here is valid for the time domain analysis of uplifting foundation response.

REFERENCES

1. Wolf J.P. and Obernhuber P.,"Non-Linear Soil-Structure-Interaction Analysis Using Green's Function of Soil in The Time Domain," Earthquake Eng. Struct. Dynamics, 13, 213-223, (1985).
2. Kawakami H. and Imamura K.,"An Analysis of Rocking Motion of Rigid Foundation with Partial Uplift Using Boundary Element Method," Journal of Struct. Engineering, 32A, 835-845, (1986)(in Japanese).
3. Pekeris C.L., "The Seismic Surface Pulse," Proc. Nat. Acad. Sci., Vol.41, 469-480, (1955).
4. Chao C.C., "Dynamic Response of An Elastic Half Space to Tangential Surface Loadings," Transa. ASME. J. Appl. Mech., Vol. 27, (1960).
5. Shimomura Y. and Tajimi H., "On An Estimation of Radiation Damping in Uplift Motions of A Base Mat Subjected to Sinusoidal Excitation" Transa. of AIJ, Vol.369, 87-101, (1986) (in Japanese).

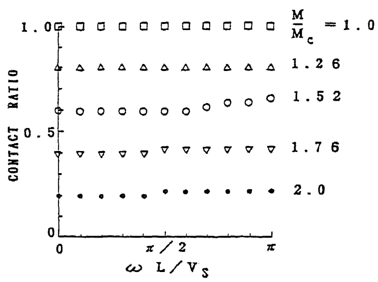

Fig.5 Relationship between excitation frequency and contact ratio

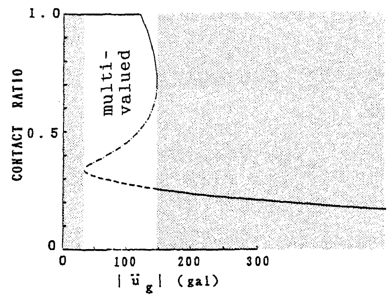

Fig.9 Example of relationship between η and $|\ddot{u}_g|$

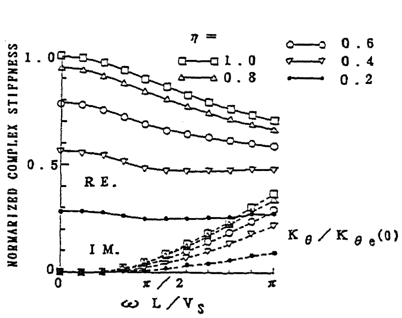

Fig.6 Equivalent complex stiffness associated with rocking mode

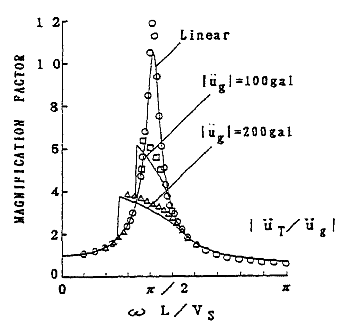

Fig.10 Magnification factor at the top of a rigid body, $|\ddot{u}_T/\ddot{u}_g|$

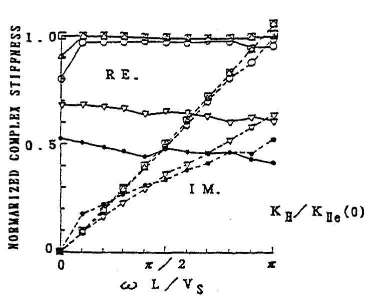

Fig.7 Equivalent complex stiffness associated with swaying mode

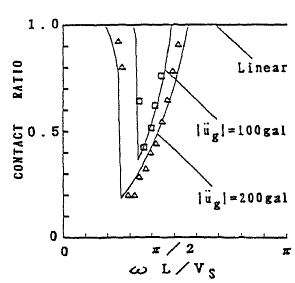

Fig.11 Contact ratio